HHS Public Access

Author manuscript

*Cell Rep*. Author manuscript; available in PMC 2022 June 16.

Published in final edited form as:

*Cell Rep*. 2022 May 10; 39(6): 110794. doi:10.1016/j.celrep.2022.110794.

# SETD4-mediated KU70 methylation suppresses apoptosis

**Yuan Wang**[1],

**Bochao Liu**[1],

**Huimei Lu**[1],

**Jingmei Liu**[1],

**Peter J. Romanienko**[2],

**Gaetano T. Montelione**[3],

**Zhiyuan Shen**[1,4,*]

[1]Department of Radiation Oncology, Rutgers Cancer Institute of New Jersey, Rutgers Robert Wood Johnson Medical School, 195 Little Albany Street, New Brunswick, NJ 08901, USA

[2]Genome Editing Shared Resource, Rutgers Cancer Institute of New Jersey, Rutgers Robert Wood Johnson Medical School, 195 Little Albany Street, New Brunswick, NJ 08901, USA

[3]Department of Chemistry and Chemical Biology, and Center for Biotechnology and Interdisciplinary Sciences, Rensselaer Polytechnic Institute, 110 8th St, Troy, NY 12180, USA

[4]Lead contact

## SUMMARY

The mammalian KU70 is a pleiotropic protein functioning in DNA repair and cytoplasmic suppression of apoptosis. We report a regulatory mechanism by which KU70's cytoplasmic function is enabled due to a methylation at K570 of KU70 by SET-domain-containing protein 4 (SETD4). While SETD4 silencing reduces the level of methylated KU70, over-expression of SETD4 enhances methylation of KU70. Mutations of Y272 and Y284 of SETD4 abrogate methylation of KU70. Although SETD4 is predominantly a nuclear protein, the methylated KU70 is enriched in the cytoplasm. SETD4 knockdown enhances staurosporine (STS)-induced apoptosis and cell killing. Over-expression of the wild-type (WT) SETD4, but not the SETD4-Y272/Y284F mutant, suppresses STS-induced apoptosis. The KU70-K570R (mouse Ku70-K568R) mutation dampens the anti-apoptosis activity of KU70. Our study identifies KU70 as a non-histone substrate



*Correspondence: shenzh@cinj.rutgers.edu.

AUTHOR CONTRIBUTIONS

Y.W. and Z.S. designed the experiments, performed data analysis, and drafted the initial version of manuscript. Y.W., B.L., H.L., J.L., and P.J.R. performed experiments. G.T.M. provided computational structural analysis. G.T.M. and P.J.R. provided revisions in the final draft of the manuscript. Z.S. directed and oversaw the project, secured funding for the study, and completed the final version of the manuscript.

SUPPLEMENTAL INFORMATION

Supplemental information can be found online at https://doi.org/10.1016/j.celrep.2022.110794.

DECLARATION OF INTERESTS

G.T.M. is a founder of the Nexomics Biosciences, and this affiliation presents no competing interests with respect to this study. The authors declare that there were no other competing interests.

of SETD4, discovers a post-translational modification of KU70, and uncovers a role for SETD4 and KU70-K570 methylation in the suppression of apoptosis.

## Graphical Abstract

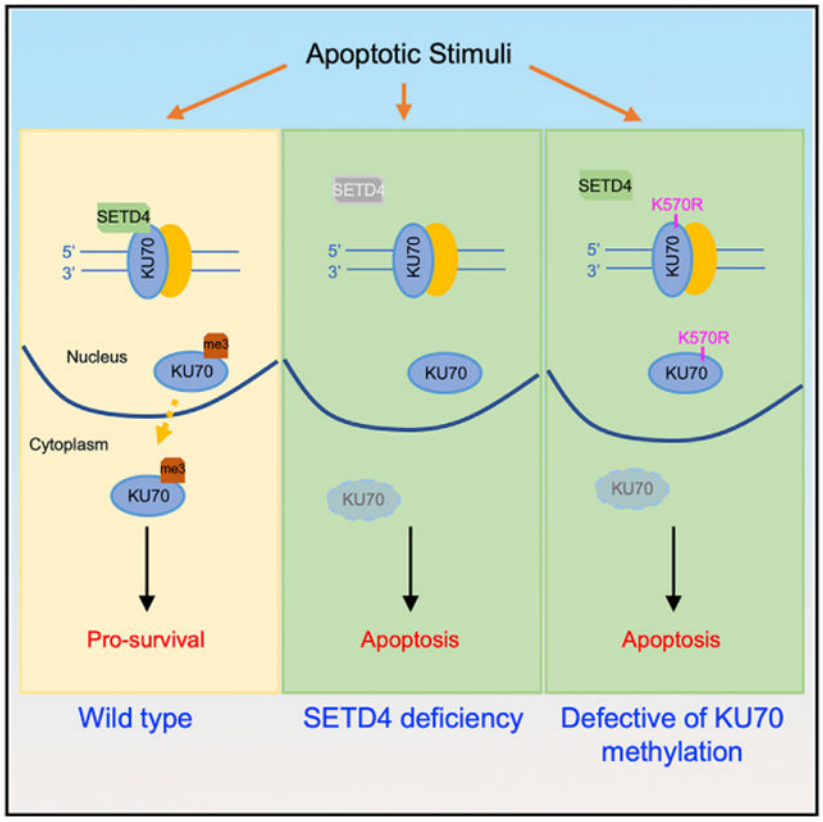


## In brief

Wang et al. identify the methylation of mammalian KU70 by SETD4. This post-translational modification is critical for KU70 localization to the cytoplasm and subsequent suppression of apoptosis.

## INTRODUCTION

Lysine methylation is a common posttranslational modification (PTM) that regulates the function of the methylated proteins (Huang and Berger, 2008). In the human genome, there are at least 57 SET-domain proteins that constitute a major group of S-adenosyl-L-methionine (AdoMet)-dependent protein lysine methyltransferases (PKMTs) (Carlson and Gozani, 2016; Petrossian and Clarke, 2011). Among the SET-domain proteins, the SETD6 group, including SETD3, SETD4, and SETD6, share about 20% amino-acid identity (Petrossian and Clarke, 2011) and have the common features of a split SET domain, with an inserted iSET region, and a substrate-binding domain similar to that of plant ribulose-1, 5-bisphosphate carboxylase/oxygenase (Rubisco) large subunit methyltransferase (LSMT). The SETD6 group of SET proteins are predicted to catalyze the methylation of non-histone

proteins due to their structural features (Petrossian and Clarke, 2011). In agreement, SETD6 has been shown to methylate lysines in several non-histone proteins (Chang et al., 2011; Feldman et al., 2019; Levy et al., 2011a, 2011b; Vershinin et al., 2020), including Rel A of nuclear factor kB (NF-kB), PLK1, and PAK, and SETD3 was recently found to methylate a histidine residue in actin (Guo et al., 2019; Kwiatkowski et al., 2018; Wilkinson et al., 2019) in addition to its function in the DNA-damage response (Abaev-Schneiderman et al., 2019).

SETD4 expression had been reported to associate with estrogen receptor (ER)-negative breast cancer cells and be involved in cell-cycle regulation (Faria et al., 2013), reduced sorafenib sensitivity of hepatocellular carcinoma (Li et al., 2014), and reduced apoptosis in androgen-independent prostate cancer cells (Zhu et al., 2016). Oncogenic fusions of SETD4 were formed with *FTCD* in invasive ductal carcinoma, *KIAA1958* in serous ovarian cancer, *B4Galt6* in lung squamous cancer, and TMPRSS2 and ERG in prostate cancers (Qingsong Gao et al., 2018; Suh et al., 2020). *Artemia* SETD4 was expressed abundantly in diapause embryos and regulated cell quiescence (Dai et al., 2017). SETD4 expression in quiescent MCF-7 breast cancer cells had been shown to maintain the stem cell population (Ye et al., 2019). We recently showed that induced *Setd4* deletion in adult mice delayed the development of radiation-induced lymphoma (Feng et al., 2020a) and sensitized bone marrow (BM) hematopoietic stem cells (HSCs) to radiation (Feng et al., 2020b). However, *Setd4* deletion can improve the BM niche function after injury (Feng et al., 2020b), consistent with the increased proliferation of BM mesenchymal stem cells (BMSCs) after *Setd4* deletion (Liao et al., 2021). Despite the cellular functional evidence for SETD4 involvement in tumorigenesis and development, an explicit knowledge about its biochemical functions, especially its authentic substrates, is lacking.

Encoded by the *XRCC6* gene, KU70 is well known for its role in non-homologous end-joining (NHEJ) repair of DNA double-strand breaks (DSBs) through heterodimerization with KU80 and recruitment of the catalytic subunit of DNA-dependent protein kinase (DNA-PKcs) to DSB sites (Falck et al., 2005; Gottlieb and Jackson, 1993; Meek et al., 2004; West et al., 1998). While KU70 is mostly localized in the nucleus, a portion of KU70 can also be found in the cytoplasm (Koike, 2002). Cytosolic KU70 has a protective function against apoptosis by binding and sequestering the proapoptotic factor BAX (Amsel et al., 2008; Cohen et al., 2004). SAF-A/B, Acinus, and PIAS (SAP) is a conserved motif found in some nuclear proteins involved in DNA repair, transcription, and RNA processing (Aravind and Koonin, 2000). While the N-terminal 538 amino acids of KU70 are involved in forming a stable heterodimer with a KU80 protein that encircles DNA, the C-terminal 51 amino acids (aa 559–609) are predicted to form a relatively independent globular structure, often referred to as the KU70-SAP domain (Anisenko et al., 2017; Hu et al., 2012; Lehman et al., 2008; Rivera-Calzada et al., 2007; Zhang et al., 2001). Between these two domains, there is a structurally flexible region (aa 539–558), referred to as the linker. It is worthwhile to point out that only the C-terminal 37 amino acids (aa 573–609) of KU70 were defined in the original SAP motif (Aravind and Koonin, 2000), and the remaining 14 amino acids (aa 559–572) appear to be specific to KU70. To distinguish them, we designate aa 573–609 as cSAP and aa 559–572 as nSAP.

Here, we report the nSAP domain of KU70 as a non-histone substrate of SETD4. This PTM activity of SETD4 enables KU70's cytoplasmic localization and is critical for KU70 to suppress apoptosis, thus potentially serving as a signaling event to coordinate the nuclear and cytoplasmic activities of KU70.

## RESULTS

### Methylation of KU70 by SETD4 *in vitro*

Human SETD4 has a predicted structure similar to human SETD3 and SETD6, including a SET domain split by an iSET region and a C-terminal Rubisco-Subs-Bind (RSB) substrate-binding domain (Figure 1A). The predicted active center of these proteins shares a critical tyrosine residue Y272 in SETD4, and SETD4 and SETD6 share another conserved tyrosine Y284 in SETD4 (Figure 1B). SETD6, SETD3, and SETD4 were suggested to comprise a distinct class of non-histone methyltransferases (Petrossian and Clarke, 2011). To explore the possibility of identifying SETD4 substrates in live cells, three independent yeast two-hybrid screens using wild-type (WT) SETD4 and the putative substrate-binding RSB domain of SETD4 as the baits were performed. We isolated 20 independent positive clones of KU70. Although these clones differed in length, they all contained the globular KU70 SAP domain, the C-terminal 51 amino acids (Figure 1C).

Using a homology model of SETD4 based on the X-ray crystal structure of human SETD3 (PDB: 3SMT; 24% sequence identity), we simulated docking between SETD4 and KU70-SAP using Rosetta-Dock (Lyskov and Gray, 2008). In the best-scoring predicted-complex structure, KU70-SAP docks between the predicted enzyme activity center and the RSB domain of SETD4 (Figure S1A). Furthermore, the side chain of K570 in KU70-nSAP resides in close proximity to the conserved residues Y272 and Y284 in the predicted activity center of SETD4 (Figure S1B). This analysis prompted us to hypothesize that the nSAP region of KU70, most likely residue K570, is a substrate of SETD4, and that Y272 and/or Y284 of the SETD4 are likely to be involved in its catalytic activity.

To test whether KU70-K570 is a substrate of SETD4, we generated and validated a series of antibodies that can recognize the methylated KU70-K570. As demonstrated in Figure S2A, our antibodies are highly specific for mono-methylated (M1), di-methylated (M2), and tri-methylated (M3) KU70 peptides. The antibodies against methylated peptides had little cross-reactivity with the M0 peptide. Then, we purified MBP-tagged SETD4 and performed an *in vitro* methylation assay using a 15-amino-acid KU70 peptide containing the K570 residue. We found that SETD4 can convert non-methylated peptide (M0) to M1, M2, and M3 peptides, the M1 peptide to M2 and M3 peptides, and the M2 peptide to M3 peptide (Figure S2B). This result strongly suggested that SETD4 indeed methylates KU70 at residue K570, which we refer to as KU70 methylation in this article.

Then, we performed an *in vitro* methylation assay using the full-length proteins of KU70/KU80 dimer. A putative SETD4 catalytic defective mutant SETD4-Y272/284F was included in this assay. As shown in Figure 1D, KU70K570me1, KU70K570me2, and KU70K570me3 were readily detectable, with the validated antibodies against methylated KU70-K570 when the KU70/KU80 were incubated with WT SETD4 but not with the SETD4-Y272/284F

mutant. These data confirmed that SETD4 can methylate KU70 at K570 *in vitro* and that Y272/Y284 of SETD4 are required, either directly or indirectly, for this methylation activity.

## Methylation of KU70 by SETD4 *in vivo*

To verify whether KU70-K570 is an authentic substrate of SETD4 in living cells, we designed experiments to deplete endogenous SETD4 in cells expressing high level of SETD4 and to over-express exogenous SETD4 in cells with a modest level of SETD4. In order to do this, we screened a panel of mammalian cells to identify cell lines with high or modest expression of endogenous SETD4 using a rabbit anti-SETD4 polyclonal antibody (h25), which was generated with recombinant SETD4 fragment (aa residues 25–100). As shown in Figure S3A, the h25 antibody detected an anticipated ~48-kDa band that can be depleted by small interfering RNA (siRNA) and short hairpin RNA (shRNA) against SETD4 (Figures 2A, S3B, and S3C).

Because H1299 cells express a high level of SETD4, while U2OS and HT1080 cells have modest levels of SETD4, we knocked down endogenous SETD4 in H1299 but over-expressed exogenous SETD4 in U2OS and HT1080 cells to test the authenticity of KU70 as an *in vivo* substrate of SETD4. As shown in Figure 2A and quantified in Figures S4A and S4B, the depletion of endogenous SETD4 by three independent siRNA or shRNAs resulted in a striking loss of KU70 tri-methylation. In support of the conclusion, we found that Myc-SETD4 over-expression in U2OS or HT1080 cells increased M3 endogenous KU70 (Figures 2B, 2C, and S4C-S4F). These results firmly demonstrated that SETD4 is required for *in vivo* KU70 K570 tri-methylation. Unlike the results from the *in vitro* methylation assay (Figure 1D), mono-methylation of KU70 was not detectable among the tested cells, and we were unable to detect di-methylation of KU70 in H1299 or U2OS cells, although an increase of M2 KU70 can be found in HT1080 cells over-expressing Myc-SETD4 (Figure 2C).

## Cytoplasmic enrichment of methylated KU70

Next, we stained H1299 cells with antibodies against total KU70 and KU70K570me3. As shown by immunofluorescence (IF) staining (Figures 3A and S5A), the signal of M3 KU70 predominantly locates in the cytoplasm, which is attenuated upon SETD4 knockdown. This suggests that M3 KU70 is enriched in the cytoplasm. To confirm this finding, we stably expressed WT Myc-SETD4 in cells with modest basal levels of endogenous SETD4 and stained for the total KU70 and M3 KU70. As represented in Figures 3B and S5B, the exogenous expression of WT SETD4 drastically increases the cytoplasmic level of M3 KU70 in U2OS cell lines. Expression of the inactive SETD4 mutants failed to enhance the level of M3 KU70 in U2OS cells (Figures 3C and S5C). The effect of SETD4 expression on KU70 tri-methylation can be verified with HT1080 (Figure S6), which is another cell line with modest endogenous SETD4 expression. However, SETD4 expression in HT1080 can also increase the level of the M2 KU70 (Figure S6C), albeit at a modest level, which is consistent with results in Figure 2C. Considering that SETD4 is predominantly a nuclear protein (Figures 3C, S6B, and S6C) but M3 KU70 is enriched in the cytoplasm, we suggest that methylation of KU70 by SETD4 likely occurs in the nucleus and that methylated KU70 is then translocated to the cytoplasm. This notion is supported by the observed cytoplasmic

re-localization of EGFP-tagged KU70-SAP domains in SETD4 over-expressing cells (Figure S6D).

## SETD4 suppresses apoptosis through KU70 methylation

Considering that KU70 is a substrate of SETD4, methylated KU70 is enriched in the cytoplasm, and cytoplasmic KU70 is known to have anti-apoptosis function (Amsel et al., 2008; Cohen et al., 2004), we next hypothesized that SETD4 may regulate apoptosis through KU70 methylation. To test this, four complementary sets of experiments were performed. First, we treated SETD4 knockdown cells with staurosporine (STS), which induces apoptosis by activating pro-apoptotic BCL2 family members without the requirement of initial DNA damage (Chechlacz et al., 2001; Cohen et al., 2004; Wei et al., 2001). We found that SETD4 depletion results in an elevated cleavage of caspase-7 (Figures 4A and S7). Second, exogenous SETD4 was overexpressed in HT1080 cells. As shown in Figures 4B and S7, WT SETD4 suppresses the STS-induced cleavage of caspase-7, but Y272F, Y284F, and Y272/284F mutants fail to suppress apoptosis. These data suggested that not only SETD4 but also its enzymatic activity is required for the anti-apoptotic activity.

Third, we developed a doxycycline (Dox)-inducible KU70 knockdown system, where the shRNA targets the 3’ UTR of KU70. KU70 and SETD4 in H1299 cells were co-depleted by Dox-induced KU70 knockdown and siSETD4 transfection. As shown in Figures 4C and S7, depletion of either KU70 or SETD4 confers a sensitization to apoptosis, while co-depletion of KU70 and SETD4 showed a similar level of apoptosis to either KU70 or SETD4 depletion alone. This implies that KU70 and SETD4 are in the same epistasis pathway for the suppression of apoptosis. Lastly, we tested whether the KU70 methylation is responsible for the anti-apoptotic activity. Several versions of Myc-EGFP-KU70 proteins were re-expressed in H1299 cells with Dox-inducible knockdown of endogenous KU70 and were treated with STS. As shown in Figures 4D, S7D, and S7H, knockdown of endogenous KU70 resulted in an elevated level of cleaved caspase-7, which can be rescued by re-expression of WT KU70. However, re-expression of the KU70-K570R mutant failed to rescue the apoptosis. These results strongly suggested that K570 is critical for the anti-apoptosis activity of KU70, consistent with the well-known fact that KU70 depletion resulted in the co-depletion of KU80 protein (Figure 4D), and this was known to be due to the stabilization of KU80 by heterodimerization with KU70 through the N terminus of KU70 (Gu et al., 1997). Interestingly, the KU70-K570R mutant has a similar activity to restore the KU80 stability as the WT KU70 (Figure 4D), but it failed to confer the anti-apoptosis activity. Furthermore, the same effect of KU70-K570R mutations on acute apoptosis induction as in H1299 cells (Figure 4D) can be observed in A549 cells (Figure S8).

## SETD4 and KU70-K570 methylation suppresses apoptosis

To assess the overall cellular sensitivity to apoptosis induction, SETD4 knockdown and over-expressing cells were exposed with varying concentrations of STS, and their relative viabilities were continuously monitored with IncuCyte time-lapse imaging for a period of 72 h. This would enable us to sensitively monitor the cell response to apoptosis induction at low concentrations of STS. A549 cells with similarly high levels of endogenous SETD4

and acute responses to STS as H1299 (Figure S8), but with WT p53, were used for the knockdown approach. The HT1080 cells with WT p53 and modest levels of endogenous SETD4 were used for the over-expression approach. As shown in Figures 5A, S9, and S10, SETD4 knockdown sensitized A549 cells to STS. On the other hand, over-expression of exogenous SETD4 confers a modest resistance to apoptosis, but the Y272/284F mutant of SETD4 fails to do so in HT1080 cells (Figures 5B, S9, and S10). To address the specific role of KU70-K570 in apoptosis, we used the same Dox-inducible KU70 knockdown in A549 cells. As shown in Figures 5C, S9, and S10, induced KU70 depletion results in sensitization to STS, and re-expression of WT KU70 rescues the sensitivity of STS, but KU70-K570R fails to do so. These results confirmed the role of KU70-K570 in suppression of apoptosis.

## KU70-K568R knockin mouse embryo fibroblasts (MEFs) are sensitive to apoptosis induction

To verify the role of KU70 methylation in mice, we replaced mouse KU70-K568 (the conserved residue corresponding to human KU70-K570) with arginine, resulting in a KU70-K568R knockin mouse line. Briefly, the CRISPR approach was used to replace AAG coding mKU70-K568 with CGC (Figure S11A). After genotyping and sequence verification (Figure S11B), germline transmission of mKU70-K568R was confirmed, and homozygous (K568R/K568R) and heterozygous (K568R/WT) mice were generated. The homozygous (K568R/K568R) and heterozygous (K568R/WT) knockin mice express equivalent levels of KU70 as WT mice (Figure S11C). It is known that depletion of KU70 destabilizes KU80 protein due to the loss of KU70/KU80 dimer (Gu et al., 1997), but the K568R mutation did not affect KU80 (Figure S11C). This was consistent with the idea that heterodimer formation between KU70 and KU80 and subsequent stabilization of each does not need the C-terminal SAP domain of KU70 and is also in agreement with the results presented in Figures 4D and S8. The knockin mice are fertile and largely normal in size at birth and during the first 90 days (Figure S11D). While additional breeding and long-term studies are underway with the knockin mice, independent MEF clones were established from embryos and used to investigate their response to apoptosis induction. As shown in Figures 5D, S9D, S9H, S10D, and S10H, homozygous K568R/K568R MEFs display more increased sensitivity to STS treatment than WT MEFs. This result suggests that the role of human KU70-K570 in the suppression of apoptosis is conserved in mouse KU70-K568 and firmly establishes the critical role of this conserved lysine residue in KU70's anti-apoptotic activity.

## KU70 methylation is a prerequisite for KU70 acetylation

Cytoplasmic KU70 is known to bind BAX through the cSAP domain, but cytoplasmic acetylation on K539 and K542 in the linker region (Figure 1C) has been shown to facilitate the release of KU70 from BAX (Cohen et al., 2004; Subramanian et al., 2005) and to allow BAX to enter mitochondria and enable apoptosis to proceed. Inhibition of deacetylases by trichostatin A (TSA) was able to enhance the level of KU70 acetylation and subsequently attenuate the cytoplasmic KU70-BAX interaction and abrogate the inhibitory activity of KU70 on apoptosis (Cohen et al., 2004). To address whether methylation-mediated KU70 cytoplasmic localization is a prerequisite of KU70 acetylation, KU70-WT or KU70-K570R were tagged with Myc-EGFP and expressed in cells. Upon treatment of the cells with TSA, tagged KU70s were immunoprecipitated (IP) and re-blotted with pan acetyl-lysine

antibody and KU70 tri-methylation antibodies, respectively. As shown in Figure 6, the level of KU70-WT acetylation in H1299 cells can be enhanced by TSA treatment, but KU70 tri-methylation is not affected by TSA. However, the KU70-K570R mutant is neither tri-methylated nor acetylated. This result was reproducible in A549 cells (Figure S12). These data are consistent with a notion that the methylation of KU70-K570 is a prerequisite for the acetylation of KU70, which reflects the fact that un-methylated KU70 cannot be enriched in the cytoplasm where KU70 acetylation and deacetylation at other lysines can occur, even though different lysine residues are subjected to cytoplasmic acetylation (Cohen et al., 2004; Subramanian et al., 2005).

## DISCUSSION

In this article, we report a non-histone substrate of SETD4, a PTM of KU70, and a mechanism by which SETD4-mediated KU70-SAP methylation suppresses apoptosis.

Like histone methylation, methylations of non-histone proteins are likely to have a critical role in functional regulation (Carlson and Gozani, 2016; Huang and Berger, 2008; Petrossian and Clarke, 2011). Among the SET proteins, SETD6 and SETD3 have the highest homologies with SETD4. The majority of the established SETD6 substrates are non-histone proteins (Chang et al., 2011; Feldman et al., 2019; Levy et al., 2011a, 2011b; Vershinin et al., 2020). Although earlier studies suggested SETD3 as a histone methyl-transferase (Eom et al., 2011; Kim et al., 2011), recent studies suggest actin to be the physiologically relevant substrate of SETD3 (Guo et al., 2019; Kwiatkowski et al., 2018; Wilkinson et al., 2019). Here, we presented strong evidence that KU70 is a non-histone substrate of SETD4, which is the third member of the SETD6 group of SET proteins. This was demonstrated not only by *in vitro* methylation assays with full-length KU70/KU80 and KU70 peptides as substrates (Figures 1D and S2B) but also with *in vivo* knockdown and over-expression approaches in live cells (Figure 2 and S4). SETD4 has been reported to methylate histone H4K20 (Dai et al., 2017; Ye et al., 2019), but H3K4 has also been reported to be a substrate (Zhong et al., 2019). Although it remains to be determined whether SETD4 has other non-histone substrate(s) or methylation site(s) in KU70, our study found that mutating a single lysine (K570 in human and K568 in mouse) in KU70 had a significant cellular phenotype, suggesting that KU70-K570 is a functionally important substate.

Largely by measuring mRNA levels, SETD4 expression was reportedly associated with a suppression of apoptosis (Li et al., 2014; Zhu et al., 2016). However, no direct cellular evidence for SETD4 to suppress apoptosis had been documented, and the accompanying mechanism had not been identified. In this study, we showed that SETD4 depletion enhanced apoptosis (Figures 4A, 4C, 5A, S9A, S9E, S10A, and S10E). Exogenous expression of WT SETD4, but not the enzymatically dead mutants, blunted apoptosis (Figures 4B, 5B, S9B, S9F, S10B, and S10F). These results not only provided clear evidence of SETD4 suppression on apoptosis but also revealed that SETD4 exerts its anti-apoptotic activity through its enzymatic activity. Although a fraction of SETD4 proteins can be observed in the cytoplasm, SETD4 is predominantly a nuclear protein (Figures 3C, S6B, and S6C). However, methylated KU70 is enriched in the cytoplasm (Figures 3 and S6A-S6C).

PTMs of KU70 by phosphorylation (Chan et al., 1999; Lee et al., 2016; Mukherjee et al., 2016), acetylation (Al Emam et al., 2018; Cohen et al., 2004; Gama et al., 2006; Subramanian et al., 2005, 2013), ubiquitination (Gama et al., 2009) (Sharma et al., 2020), and sumoylation in yeast (Hang et al., 2014) had been previously reported. However, there has been no previous report of KU70 methylation nor PTM in the mammalian KU70-SAP domain. Here, we report a modification of KU70 within the SAP domain. We showed that a single amino-acid change in human KU70-K570 or mouse KU70-K568 has a striking impact on KU70's anti-apoptotic activity. These results underscore a critical role of KU70 methylation in its anti-apoptosis activity.

In a structural model (Rivera-Calzada et al., 2007; Walker et al., 2001), the C-terminal globular KU70-SAP (aa 559–609) domain is linked to the KU70/KU80 dimer structure by a flexible linker region of KU70 (aa 539–558). While the linker region and the KU70-SAP are not a part of the core KU70/KU80 dimer that encircles the DNA, they look like a hand reaching out from the main body of the KU70/KU80 dimer, with the linker region as the flexible "arm" and the KU70-SAP as a "fist" touching back to another part of the core KU70/KU80 dimer. It was suggested that this conformation may stabilize the KU70/KU80 dimer in its DNA-binding form (Rivera-Calzada et al., 2007). Interestingly, the KU70-nSAP and particularly K570 are part of the surface in contact with KU80 of the core KU70/KU80 dimer. This raises a possibility that the methylation of KU70 at K570 may affect the stability of the core KU70/KU80 dimer, or trigger the disassociation of KU70/KU80 dimer, to form a KU70 conformation and enable KU70 export into the cytoplasm. Furthermore, SETD4 is predominantly a nuclear protein, but methylated KU70 is enriched in the cytoplasm. Thus, nuclear KU70 methylation and its subsequent disassociation from KU80 and re-location to the cytoplasm may serve as a signaling event to coordinate the completion of DSB repair in the nucleus and the accompanying pro-survival outcome in cytoplasm, thus playing a critical role in cell-fate determination after DNA damage.

In this article, we also showed that KU70 methylation is a prerequisite for KU70 localization to the cytoplasm and subsequent suppression of apoptosis. It was known that the anti-apoptotic activity of unacetylated KU70 was mediated by its interaction with cytosolic BAX to restrain BAX from entering mitochondria (Amsel et al., 2008; Cohen et al., 2004; Sawada et al., 2003; Subramanian et al., 2005), and degradation of cytosolic KU70 promoted apoptosis (Gama et al., 2009). It had also been reported that cytoplasmic KU70 acetylation in the linker region, especially at residues K539 and K542, can dampen the KU70 and BAX interaction (Cohen et al., 2004; Subramanian et al., 2013), but deacetylation of KU70 at these sites can restore the KU70-BAX interaction (Chen et al., 2007; Subramanian et al., 2005, 2011). A logical question is whether there is a sequential order of KU70 methylation and acetylation. In our study, we measured the levels of acetylated and methylated KU70 upon expression of the KU70 WT or the K570R mutant in cells. We found significantly reduced acetylation of overall KU70 when KU70-K570 is mutated (Figures 6 and S12), suggesting that KU70-K570 methylation likely precedes acetylation. This is consistent with a model in which methylated KU70 is disassociated from KU dimers and translocates to the cytoplasm, where KU70 can be acetylated or deacetylated to fine-tune its activity in suppressing apoptosis.

In summary, our study provided the experimental evidence that SETD4 has a non-histone methyltransferase activity and underscored the critical role of a KU70 modification in its anti-apoptotic role. Future studies are needed to address whether this KU70 modification plays a role in KU70's nuclear function as well.

### Limitations of the study

Our study has demonstrated that residue K570 of human KU70 is a methylation substrate by SETD4 and revealed a non-histone methyltransferase activity of SETD4. We mainly resorted to hypothesis-driven and targeted approaches to reach these conclusions. Thus, our study offers little information on whether SETD4 has other non-histone substrate(s) and whether KU70 can be methylated at additional site(s) beside K570. A comprehensive methylation analysis preferably including the KU70-K570R mutant as the substrate and more quantitative methylation detections would be desirable to determine whether there are other lysine methylation sites and to confirm which methylation status (mono-, di-, or tri-) is the main form of modification *in vivo*. Furthermore, our findings are mainly related to the anti-apoptosis activity of KU70, but we have not yet offered any insight on whether this methylation affects the nuclear activity of KU70 especially in DNA repair.

## STAR★METHODS

### RESOURCE AVAILABILITY

**Lead contact—**Further information and requests for resources and reagents should be directed to and will be fulfilled by the lead contact, Zhiyuan Shen (shenzh@cinj.rutgers.edu).

**Materials availability—**All unique/stable reagents generated in this study are available from the lead contact with a completed Materials Transfer Agreement.

### Data and code availability

- This paper analyzes existing, publicly available data. The accession numbers for the datasets are listed in the key resources table.
- All data reported in this paper will be shared by the lead contact upon request.
- This paper does not report original code.
- Any additional information required to reanalyze the data reported in this paper is available from the lead contact upon request.

### EXPERIMENTAL MODEL AND SUBJECT DETAILS

**Mouse models—**All mouse work and procedures were approved by the Institutional Animal Care and Use Committee at Rutgers Robert Johnson Medical School. In addition, all animal experiments were performed in accordance with relevant guidelines and regulations. Ku70-K568R knock-in mice were bred on a C57/BL6 background, with ages ranging from E15.5 embryo to 3-month-old from both genders. Animals were housed at 12 hours light/

dark cycle in ventilated cages with controlled temperature and humidity. Water and standard mouse diet were provided ad libitum, and bedding changed regularly.

**Cell lines—**Different human cell lines, HT1080, U2OS, HepG2, H1299, A549, MCF-7, HeLa and HEK293 were grown in α- Minimum Essential Medium with 10% fetal bovine serum, 20 mM glutamine and 1% penicillin-streptomycin at 37°C containing 5% $CO_2$ incubator. Primary cell lines used in this study were isolated from Ku70-WT/K568R knock-in mouse (3-month-old female). Mouse embryonic fibroblasts (MEFs) Ku70-WT/WT and KU70-K568R/K568R were isolated from E15.5 embryos of littermates upon cross between heterozygous Ku70-WT/K568R mice (3-month-old males) and Ku70-WT/K568R (3-month-old females).

## METHOD DETAILS

**Generation of antibodies—**The rabbit anti-SETD4 was made using 25–100 amino acids of human SETD4 (hSETD4) as antigen and purified by high-performance liquid chromatography. For rabbit anti-Ku70 methylation antibodies, peptides (559-YSEEELKTHISKGTLGKFT) that correspond to amino acids 559–577 of KU70 with lysine (mono-, di- or tri-) methylation at position 570 were synthesized and purified by Syd Labs Inc. The sources of commercial primary antibodies are listed in the key resources table.

**Recombinant protein expression for *in vitro* methylation reactions—**WT or mutant of hSETD4 was cloned into pMAL-c2X vector containing N-terminal MBP fusion. Then full length hSETD4 was expressed in Rosetta (DE3) strain of bacteria overnight at 20°C in the presence of 0.1 mM IPTG and purified by amylose resin according to the manufacturer's recommendations. 2 μg of WT or mutant SETD4 and 800 ng KU70 peptides containing K570 methylation residue, or 4 mg of purified KU70/80 dimer protein as substrate were incubated in 10×HMT buffer supplemented with 0.16 mmol/L SAM (S-adenosylmethionine, as the donor methyl group). For the controls, only KU70/80 dimer was added. Recombinant SET7 was used as a positive control to test H3 and H4 methylation. The total volume of a reaction mixture was adjusted to 50 μL. The samples were incubated at 30° C for 2 h and 65°C for 20 min. Then the samples were added with SDS sample loading buffer and subjected to western blots analysis.

**Plasmid vectors and production of retroviruses and lentiviruses—**The WT or mutant cDNA of hSETD4 was cloned into the pLXSH vector (hygromycin B selection) and the WT or mutant cDNA of hKU70 was cloned into the pLXSP vector (puromycin selection) and used to produce retrovirus, respectively. To enable stable expression of cDNA transgenes, cells were infected with retrovirus by three cycles of 8 h infection and 16 h of incubation with fresh medium, and then subjected to 50 μg/mL hygromycin B or 1 μg/mL puromycin selection. Positive single and mixed clones were obtained, and the population was expanded to provide stable cell lines. The SETD4 and KU70 mutants were generated with a site-directed mutagenesis kit.

To construct inducible KU70 knockdown, KU70 shRNA which targets 3'-UTR of the KU70 were cloned into the Tet-pLKO-Neo vector through the Age I and EcoR I sites. To generate

lentiviruses, 293T cells were co-transfected with pLKO-shKU70-Neo, psPAX2 and pMD2G in the ratio 2:1:1. After 72 hrs post the transfection, virus-containing supernatant was collected, filtered through a 0.45 μm nylon mesh and infected target cells H1299 and A549 with 8 μg/mL polybrene twice. After infection, the cells were allowed to recover in the fresh medium overnight, and then selected in neomycin (800 μg/mL) for 5 days.

**Knock down of SETD4 by small interfering RNA transfection—**H1299 or A549 cells were transfected with siRNA against SETD4 using the same sequence as reported (Ye et al., 2019) (si-SETD4: 5'- GAGGGCUGAUGAGUCAAACAU-3') to knock down endogenous SETD4 gene. At post-transfection 48–72 h, cell extracts were collected for western blots and IF staining. The scrambled siRNA (scrRNA: 5'-UUCGAACGUGUCACGU CAA-3') was used as the non-silencing control.

**Western blotting and Co-immunoprecipitation (co-IP)—**To perform western blots, cells were lysed in RIPA buffer (50 mM Tris HCl, pH 7.4, with 150 mM NaCl, 1 mM EDTA, and 1% Triton X-100, 0.1% SDS, 0.1% sodium deoxycholate) supplemented with protease inhibitors (1 mM Leupeptin, 1 mM Aprotinin, 20 mM PMSF) and sonicated. Lysates were subjected to PAGE electrophoresis and transferred to nitrocellulose membrane. The membranes were blocked in 5% milk for 1 hr at room temperature and incubated with the specific antibodies at 4°C overnight. Following incubation, membranes were washed three times in 0.1% Tween-20-TBS and incubated at room temperature for 1 hr with HRP anti-mouse or anti-rabbit IgG secondary antibodies. Membranes were then washed as described above and proteins were detected using ECL western blotting substrate.

To perform co-IP, cells were lysed in lysis buffer (0.1% IGEPAL CA-630, 50 mM Tris HCl, pH 7.4, 50 mM NaCl, 2 mM DTT) supplemented with protease inhibitor (1 mM Leupeptin, 1 mM Aprotinin, 20 mM PMSF), sonicated and centrifuged at 13,000 rpm for 15 min at 4°C. Supernatants were immunoprecipitated with anti-Myc affinity beads overnight at 4°C with constant rotation. Beads were then washed with cold lysis buffer at 4°C for three times, then resuspended in lysis buffer with SDS sample loading buffer, boiled for 5 min, and subject to western blot analysis. Three independent co-IP experiments were performed for each sample to ensure reproducibility.

**Immunofluorescence (IF) staining—**Cells grown on cover slips or chamber slides were fixed with Formalde-Fresh Solution for 15 min and then permeabilized with 0.15% Triton X-100 for 15 min. After washing with PBS three times, fixed cells were blocked with 2% BSA at room temperature for 1 hr, then incubated with primary antibodies at 4°C overnight. Samples were then washed with PBS three times, and then incubated with FITC or TRITC conjugated anti-mouse or anti-rabbit secondary antibodies at room temperature for 1 hr. Nuclei were visualized by DNA staining with DAPI mounting medium.

**Creation of KU70 knock-in mice by CRISPR and IVF—**A KU70-K568R knock in mouse line was generated using a single gRNA and a mixture of two templates adjacent to the CAS cutting site. Briefly, the WT mouse KU70 nucleotide and amino acid sequences starting with E556, and the sequence of K568R mouse line which the AAG in the WT KU70 was replaced with CGC coding Arginine. This also led to the creation of a AciI site

(C^CGC; or GCG^G on opposing strand, blue highlighted in Figure S7A) to be used for genotyping. Mice were housed in individually ventilated cages in a specific pathogen-free facility on a 12 hrs light/dark cycle with *ad libitum* access to food and water. The animal works presented in this study were approved by the Institutional Animal Care and Use Committee at Rutgers Robert Johnson Medical School. We adhered to and followed our institutional guideline regarding to animal welfare issues.

**Generation of MEF cell lines from Ku70-K568R knock-in mouse model—**Ku70-WT/K568R pregnant female mouse (3-month-old) was euthanized to harvest the embryos (E15.5), which were separated by slicing through the uterus in the regions between each embryo. The skin from the whole back of each embryo was teared off and minced using a sterile scissors, then placed in 0.25% Trypsin-EDTA solution and enzymatically digested at 37°C for 30 min with shaking at 10 mins intervals. The α-Minimum Essential Medium with 10% fetal bovine serum was added to inactivate the trypsin, and mixed in the tube. After the cell suspension was sat for about 5 mins to allow larger embryo fragments to sink to the bottom of the tube. The supernatant consisting of single cells was transferred to a new tube, and then centrifuged at 1,000 rpm for 3 min. The cell pellet was resuspended in α-Minimum Essential Medium with 10% fetal bovine serum, 20 mM glutamine and 1% penicillinstreptomycin, and cultured in 10 cm petri dish at 37°C containing 5% $CO_2$ incubator.

**Structural modeling of KU70-SAP and SETD4 interaction—**The KU70-SAP structure was based on PDB 1JJR (Zhang et al., 2001), and the predicted SETD4 structure was homology modeled based on the three-dimensional structure of human SETD3 (PDB ID 3SMT; 24% sequence identity, e-val: 1E-12) using the web-based I-TASSER server ver 3.0 (https://zhanggroup.org/I-TASSER/) (Roy et al., 2010). The docking model was generated with the web-based RosettaDock server ver 3.2 (https://www.rosettacommons.org/software/servers) (Gray et al., 2003; Lyskov and Gray, 2008) using a flexible ligand docking protocol. Three-dimensional coordinates for S-adenosyl methionine (SAM) were obtained from the Protein Data Bank (PDB) (http://www.rcsb.org). In this approach, an Interface Score (I-sc) between −5 and −10 are considered a good fit (Gray et al., 2003; Lyskov and Gray, 2008). Meeting this criterium are three docking models with I-sc scores of −7.17, −6.98, and −8.13 respectively. These also happen to have the lowest total scores and can be superimposed very well. The model with the best I-sc values was used in this report (Figure S1). SAM was docked into the model of the KU70-SAP/SETD4 complex using the AutoDock Vina Ver 4 suite (Trott and Olson, 2010). Protein and ligand coordinates were prepared, and all docking simulations were analyzed, using AutoDock Tools (Sanner, 1999). Atomic coordinates for the best conformation obtained in each docking simulation were saved in PDB format for analysis. The protein-ligand complexes were analyzed in detail using the open source PyMol ver 2.0 (https://pymol.org/2/) molecular visualization tool (DeLano, 2009).

## QUANTIFICATION AND STATISTICAL ANALYSIS

Statistical analyses of the data were performed using the methods as described in the figure legends. In Figure 5: Results were average of at least six independent experiments. Error bars, SEM. p values were calculated based on two-tailed *Student t*-test. In Figures S4, S7,

S9, and S10: Each result was average of 3 independent experiments. Error bars, SEM. Two-tailed *t*-test was used for calculating p values. *p < 0.05, **p < 0.01, ***p < 0.001/ In Figure S5: More than 50 cells were measured in each sample. Error bars, SEM. Two-tailed *t*-test was used for statistical analysis. ***p < 0.001. In Figure S11D: Body weight was presented as averages and their standard errors (SEM), and the exact number of animals for KU70 knock-in mouse model is provided in the figure. The number of replicates and measures of significance are present in the figure legends and denoted in the figures.

## Supplementary Material

Refer to Web version on PubMed Central for supplementary material.

## ACKNOWLEDGMENTS

This research was supported by NIH R01CA195612, NIH R01CA260724, NIH P01CA250957, and NJCCR DCHS20CRF002 to Z.S., by NJCCR DCHS19PPC011 to Y.W., by NIH R35GM141818 to G.T.M., and by the Genome Editing Shared Resources of The Rutgers Cancer Institute of New Jersey (P30CA072720). Z.S. acknowledges the support of the Robert Wood Johnson Foundation to the Rutgers Cancer Institute of New Jersey. We thank Drs. Shijie Lan and Yanying Huo for assistance at the early stage of this study and Dr. Rongjin Guan for assistance on structural modeling.

## REFERENCES

Abaev-Schneiderman E, Admoni-Elisha L, and Levy D (2019). SETD3 is a positive regulator of DNA-damage-induced apoptosis. Cell Death Dis. 10, 74. 10.1038/s41419-019-1328-4. [PubMed: 30683849]

Al Emam A, Arbon D, Jeeves M, and Kysela B (2018). Ku70 N-terminal lysines acetylation/deacetylation is required for radiation-induced DNA-double strand breaks repair. Neoplasma 65, 708–719. 10.4149/neo_2018_171020n673. [PubMed: 30249103]

Amsel AD, Rathaus M, Kronman N, and Cohen HY (2008). Regulation of the proapoptotic factor Bax by Ku70-dependent deubiquitylation. Proc. Natl. Acad. Sci. U S A 105, 5117–5122. 10.1073/pnas.0706700105. [PubMed: 18362350]

Anisenko AN, Knyazhanskaya ES, Zatsepin TS, and Gottikh MB (2017). Human Ku70 protein binds hairpin RNA and double stranded DNA through two different sites. Biochimie 132, 85–93. 10.1016/j.biochi.2016.11.001. [PubMed: 27825805]

Aravind L, and Koonin EV (2000). SAP – a putative DNA-binding motif involved in chromosomal organization. Trends Biochem. Sci 25, 112–114. 10.1016/s0968-0004(99)01537-6. [PubMed: 10694879]

Carlson SM, and Gozani O (2016). Nonhistone lysine methylation in the regulation of cancer pathways. Cold Spring Harb. Perspect. Med 6, a026435. 10.1101/cshperspect.a026435. [PubMed: 27580749]

Chan DW, Ye R, Veillette CJ, and Lees-Miller SP (1999). DNA-dependent protein kinase phosphorylation sites in Ku 70/80 heterodimer. Biochemistry 38, 1819–1828. 10.1021/bi982584b. [PubMed: 10026262]

Chang Y, Levy D, Horton JR, Peng J, Zhang X, Gozani O, and Cheng X (2011). Structural basis of SETD6-mediated regulation of the NF-kB network via methyl-lysine signaling. Nucleic Acids Res. 39, 6380–6389. 10.1093/nar/gkr256. [PubMed: 21515635]

Chechlacz M, Vemuri MC, and Naegele JR (2001). Role of DNA-dependent protein kinase in neuronal survival. J. Neurochem 78, 141–154. 10.1046/j.1471-4159.2001.00380.x. [PubMed: 11432981]

Chen CS, Wang YC, Yang HC, Huang PH, Kulp SK, Yang CC, Lu YS, Matsuyama S, Chen CY, and Chen CS (2007). Histone deacetylase inhibitors sensitize prostate cancer cells to agents that produce DNA double-strand breaks by targeting Ku70 acetylation. Cancer Res. 67, 5318–5327. 10.1158/0008-5472.can-06-3996. [PubMed: 17545612]

Cohen HY, Lavu S, Bitterman KJ, Hekking B, Imahiyerobo TA, Miller C, Frye R, Ploegh H, Kessler BM, and Sinclair DA (2004). Acetylation of the C terminus of Ku70 by CBP and PCAF controls bax mediated apoptosis. Mol. Cell 13, 627–638. 10.1016/s1097-2765(04)00094-2. [PubMed: 15023334]

Dai L, Ye S, Li HW, Chen DF, Wang HL, Jia SN, Lin C, Yang JS, Yang F, Nagasawa H, and Yang WJ (2017). SETD4 regulates cell quiescence and catalyzes the trimethylation of H4K20 during diapause formation in Artemia. Mol. Cell. Biol 37. 10.1128/mcb.00453-16.

DeLano (2009). The PyMOL Molecular Graphics System, Version 2.0 (Schrödinger, LLC.).

Eom GH, Kim KB, Kim JH, Kim JY, Kim JR, Kee HJ, Kim DW, Choe N, Park HJ, Son HJ, et al. (2011). Histone methyltransferase SETD3 regulates muscle differentiation. J. Biol. Chem 286, 34733–34742. 10.1074/jbc.m110.203307. [PubMed: 21832073]

Falck J, Coates J, and Jackson SP (2005). Conserved modes of recruitment of ATM, ATR and DNA-PKcs to sites of DNA damage. Nature 434, 605–611. 10.1038/nature03442. [PubMed: 15758953]

Faria JAQA, Corrêa NCR, de Andrade C, de Angelis Campos AC, dos Santos Samuel de Almeida R, Rodrigues TS, de Goes AM, Gomes DA, and Silva FP (2013). SET domain-containing protein 4 (SETD4) is a newly identified cytosolic and nuclear lysine methyltransferase involved in breast cancer cell proliferation. J. Cancer Sci. Ther 5, 58–65. [PubMed: 24738023]

Feldman M, Vershinin Z, Goliand I, Elia N, and Levy D (2019). The methyltransferase SETD6 regulates Mitotic progression through PLK1 methylation. Proc. Natl. Acad. Sci. U S A 116, 1235–1240. 10.1073/pnas.1804407116. [PubMed: 30622182]

Feng X, Lu H, Yue J, Schneider N, Liu J, Denzin LK, Chan CS, De S, and Shen Z (2020a). Loss of Setd4 delays radiation-induced thymic lymphoma in mice. DNA Repair (Amst) 86, 102754. 10.1016/j.dnarep.2019.102754. [PubMed: 31794893]

Feng X, Lu H, Yue J, Shettigar M, Liu J, Denzin LK, and Shen Z (2020b). Deletion of mouse Setd4 promotes the recovery of hematopoietic failure. Int. J. Radiat. Oncol. Biol. Phys 107, 779–792. 10.1016/j.ijrobp.2020.03.026. [PubMed: 32259569]

Gama V, Gomez JA, Mayo LD, Jackson MW, Danielpour D, Song K, Haas AL, Laughlin MJ, and Matsuyama S (2009). Hdm2 is a ubiquitin ligase of Ku70-Akt promotes cell survival by inhibiting Hdm2-dependent Ku70 destabilization. Cell Death Differ. 16, 758–769. 10.1038/cdd.2009.6. [PubMed: 19247369]

Gama V, Yoshida T, Gomez JA, Basile DP, Mayo LD, Haas AL, and Matsuyama S (2006). Involvement of the ubiquitin pathway in decreasing Ku70 levels in response to drug-induced apoptosis. Exp. Cell Res 312, 488–499. 10.1016/j.yexcr.2005.11.016. [PubMed: 16368436]

Gottlieb TM, and Jackson SP (1993). The DNA dependent protein kinase requirement for DNA ends and association with Ku antigen. Cell 72, 131–142. 10.1016/0092-8674(93)90057-w. [PubMed: 8422676]

Gray JJ, Moughon S, Wang C, Schueler-Furman O, Kuhlman B, Rohl CA, and Baker D (2003). Protein-protein docking with simultaneous optimization of rigid-body displacement and side-chain conformations. J. Mol. Biol 331, 281–299. 10.1016/s0022-2836(03)00670-3. [PubMed: 12875852]

Gu Y, Seidl KJ, Rathbun GA, Zhu C, Manis JP, Stanhope-Baker P, Schlissel MS, Roth DB, Alt FW, van der Stoep N, et al. (1997). Growth retardation and leaky SCID phenotype of Ku70-deficient mice. Immunity 7, 653–665. 10.1016/s1074-7613(00)80386-6. [PubMed: 9390689]

Guo Q, Liao S, Kwiatkowski S, Tomaka W, Yu H, Wu G, Tu X, Min J, Drozak J, and Xu C (2019). Structural insights into SETD3-mediated histidine methylation on beta-actin. Elife 8. 10.7554/elife.43676.

Hang LE, Lopez CR, Liu X, Williams JM, Chung I, Wei L, Bertuch AA, and Zhao X (2014). Regulation of Ku-DNA association by Yku70 C-terminal tail and SUMO modification. J. Biol. Chem 289, 10308–10317. 10.1074/jbc.m113.526178. [PubMed: 24567323]

Hu S, Pluth JM, and Cucinotta FA (2012). Putative binding modes of Ku70-SAP domain with double strand DNA: a molecular modeling study. J. Mol. Model 18, 2163–2174. 10.1007/s00894-011-1234-x. [PubMed: 21947447]

Huang J, and Berger SL (2008). The emerging field of dynamic lysine methylation of non-histone proteins. Curr. Opin. Genet. Dev 18, 152–158. 10.1016/j.gde.2008.01.012. [PubMed: 18339539]

Kim DW, Kim KB, Kim JY, and Seo SB (2011). Characterization of a novel histone H3K36 methyltransferase setd3 in zebrafish. Biosci. Biotechnol. Biochem 75, 289–294. 10.1271/bbb.100648. [PubMed: 21307598]

Koike M (2002). Dimerization, translocation and localization of Ku70 and Ku80 proteins. J. Radiat. Res 43, 223–236. 10.1269/jrr.43.223. [PubMed: 12518983]

Kwiatkowski S, Seliga AK, Vertommen D, Terreri M, Ishikawa T, Grabowska I, Tiebe M, Teleman AA, Jagielski AK, Veiga-da-Cunha M, and Drozak J (2018). SETD3 protein is the actin-specific histidine N-methyl-transferase. Elife 7. 10.7554/elife.37921.

Lee KJ, Saha J, Sun J, Fattah KR, Wang SC, Jakob B, Chi L, Wang SY, Taucher-Scholz G, Davis AJ, and Chen DJ (2016). Phosphorylation of Ku dictates DNA double-strand break (DSB) repair pathway choice in S phase. Nucleic Acids Res. 44, 1732–1745. 10.1093/nar/gkv1499. [PubMed: 26712563]

Lehman JA, Hoelz DJ, and Turchi JJ (2008). DNA-dependent conformational changes in the Ku heterodimer. Biochemistry 47, 4359–4368. 10.1021/bi702284c. [PubMed: 18355052]

Levy D, Kuo AJ, Chang Y, Schaefer U, Kitson C, Cheung P, Espejo A, Zee BM, Liu CL, Tangsombatvisit S, et al. (2011a). Lysine methylation of the NF-κB subunit RelA by SETD6 couples activity of the histone methyltransferase GLP at chromatin to tonic repression of NF-κB signaling. Nat. Immunol 12, 29–36. 10.1038/ni.1968. [PubMed: 21131967]

Levy D, Liu CL, Yang Z, Newman AM, Alizadeh AA, Utz PJ, and Gozani O (2011b).A proteomic approach for the identification of novel lysine methytransferase substrates. Epigenet. Chromatin 4, 19.

Li G-M, Wang Y-G, Pan Q, Wang J, Fan J-G, and Sun C (2014). RNAi screening with shRNAs against histone methylation-related genes reveals determinants of methylation-related genes reveals determinants of sorafenib snsitivity in hepatocellular carcinoma cells. Int. J. Clin. Exp. Pathol, 1085–1092. [PubMed: 24696725]

Liao X, Wu C, Shao Z, Zhang S, Zou Y, Wang K, Ha Y, Xing J, Zheng A, Shen Z, et al. (2021). SETD4 in the proliferation, migration, angiogenesis, myogenic differentiation and genomic methylation of bone marrow mesenchymal stem cells. Stem Cell Rev. Rep 17, 1374–1389. 10.1007/s12015-021-10121-1. [PubMed: 33506343]

Lyskov S, and Gray JJ (2008). The RosettaDock server for local protein-protein docking. Nucleic Acids Res. 36, W233–W238. 10.1093/nar/gkn216. [PubMed: 18442991]

Meek K, Gupta S, Ramsden DA, and Lees-Miller SP (2004). The DNA-dependent protein kinase: the director at the end. Immunol. Rev 200, 132–141. 10.1111/j.0105-2896.2004.00162.x. [PubMed: 15242401]

Mukherjee S, Chakraborty P, and Saha P (2016). Phosphorylation of Ku70 subunit by cell cycle kinases modulates the replication related function of Ku heterodimer. Nucleic Acids Res. 44, 7755–7765. 10.1093/nar/gkw622. [PubMed: 27402161]

Petrossian TC, and Clarke SG (2011). Uncovering the human methyltrans-ferasome. Mol. Cell. Proteomics 10, M110.000976. 10.1074/mcp.m110.000976.

Qingsong Gao W-WL, Jayasinghe RG, Cao S, Liao WW, Reynolds SM, Wyczalkowski MA, Yao L, Yu L, Sun SQ, Chen K, et al. (2018). Driver fusions and their implications in the development and treatment of human cancers. Cell Rep. 23, 227–238. 10.1016/j.celrep.2018.03.050. [PubMed: 29617662]

Rivera-Calzada A, Spagnolo L, Pearl LH, and Llorca O (2007). Structural model of full-length human Ku70-Ku80 heterodimer and its recognition of DNA and DNA-PKcs. EMBO Rep. 8, 56–62. 10.1038/sj.embor.7400847. [PubMed: 17159921]

Roy A, Kucukural A, and Zhang Y (2010). I-TASSER: a unified platform for automated protein structure and function prediction. Nat. Protoc 5, 725–738. 10.1038/nprot.2010.5. [PubMed: 20360767]

Sanner MF (1999). Python: a programming language for software integration and development. J. Mol. Graph. Model 17, 57–61. [PubMed: 10660911]

Sawada M, Sun W, Hayes P, Leskov K, Boothman DA, and Matsuyama S (2003). Ku70 suppresses the apoptotic translocation of Bax to mitochondria. Nat. Cell Biol 5, 320–329. 10.1038/ncb950. [PubMed: 12652308]

Sharma A, Alswillah T, Kapoor I, Debjani P, Willard B, Summers MK, Gong Z, and Almasan A (2020). USP14 is a deubiquitinase for Ku70 and critical determinant of non-homologous end joining repair in autophagy and PTEN-deficient cells. Nucleic Acids Res. 48, 736–747. 10.1093/nar/gkz1103. [PubMed: 31740976]

Subramanian C, Hada M, Opipari AW Jr., Castle VP, and Kwok RP (2013). CREB-binding protein regulates Ku70 acetylation in response to ionization radiation in neuroblastoma. Mol. Cancer Res 11, 173–181. 10.1158/1541-7786.mcr-12-0065. [PubMed: 23223795]

Subramanian C, Jarzembowski JA, Opipari AW Jr., Castle VP, and Kwok RP (2011). HDAC6 deacetylates Ku70 and regulates Ku70-Bax binding in neuroblastoma. Neoplasia 13, 726–734. 10.1593/neo.11558. [PubMed: 21847364]

Subramanian C, Opipari AW Jr., Bian X, Castle VP, and Kwok RPS (2005). Ku70 acetylation mediates neuroblastoma cell death induced by histone deacetylase inhibitors. Proc. Natl. Acad. Sci. U S A 102, 4842–4847. 10.1073/pnas.0408351102. [PubMed: 15778293]

Suh J, Jeong CW, Choi S, Ku JH, Kim HH, Kim KS, and Kwak C (2020). Targeted next-generation sequencing for locally advanced prostate cancer in the Korean population. Investig. Clin. Urol 61, 127–135. 10.4111/icu.2020.61.2.127.

Trott O, and Olson AJ (2010). AutoDock Vina: improving the speed and accuracy of docking with a new scoring function, efficient optimization, and multithreading. J. Comput. Chem 31, 455–461. 10.1002/jcc.21334. [PubMed: 19499576]

Vershinin Z, Feldman M, and Levy D (2020). PAK4 methylation by the methyltransferase SETD6 attenuates cell adhesion. Sci. Rep 10, 17068. 10.1038/s41598-020-74081-1. [PubMed: 33051544]

Walker IH, Hsieh PC, and Riggs PD (2010). Mutations in maltose-binding protein that alter affinity and solubility properties. Appl. Microbiol. Biotechnol 88, 187–197. 10.1007/s00253-010-2696-y. [PubMed: 20535468]

Walker JR, Corpina RA, and Goldberg J (2001). Structure of the Ku heterodimer bound to DNA and its implications for double-strand break repair. Nature 412, 607–614. 10.1038/35088000. [PubMed: 11493912]

Wei MC, Zong WX, Cheng EHY, Lindsten T, Panoutsakopoulou V, Ross AJ, Roth KA, MacGregor GR, Thompson CB, and Korsmeyer SJ (2001). Proapoptotic BAX and BAK: a requisite gateway to mitochondrial dysfunction and death. Science 292, 727–730. 10.1126/science.1059108. [PubMed: 11326099]

West RB, Yaneva M, and Lieber MR (1998). Productive and nonproductive complexes of Ku and DNA dependent protein kinase at DNA termini. Mol. Cell. Biol 18, 5908–5920. 10.1128/mcb.18.10.5908. [PubMed: 9742108]

Wiederschain D, Susan W, Chen L, Loo A, Yang G, Huang A, Chen Y, Caponigro G, Yao YM, Lengauer C, et al. (2009). Single-vector inducible lentiviral RNAi system for oncology target validation. Cell Cycle 8, 498–504. 10.4161/cc.8.3.7701. [PubMed: 19177017]

Wilkinson AW, Diep J, Dai S, Liu S, Ooi YS, Song D, Li TM, Horton JR, Zhang X, Liu C, et al. (2019). SETD3 is an actin histidine methyltransferase that prevents primary dystocia. Nature 565, 372–376. 10.1038/s41586-018-0821-8. [PubMed: 30626964]

Ye S, Ding YF, Jia WH, Liu XL, Feng JY, Zhu Q, Cai SL, Yang YS, Lu QY, Huang XT, et al. (2019). SET domain-containing protein 4 epigenetically controls breast cancer stem cell quiescence. Cancer Res. 79, 4729–4743. 10.1158/0008-5472.can-19-1084. [PubMed: 31308046]

Zhang Z, Zhu L, Lin D, Chen F, Chen DJ, and Chen Y (2001). The three-dimensional structure of the C-terminal DNA-binding domain of human Ku70. J. Biol. Chem 276, 38231–38236. 10.1074/jbc.m105238200. [PubMed: 11457852]

Zhong Y, Ye P, Mei Z, Huang S, Huang M, Li Y, Niu S, Zhao S, Cai J, Wang J, et al. (2019). The novel methyltransferase SETD4 regulates TLR agonist-induced expression of cytokines through methylation of lysine 4 at histone 3 in macrophages. Mol. Immunol 114, 179–188. 10.1016/j.molimm.2019.07.011. [PubMed: 31376731]

Zhu S, Xu Y, Song M, Chen G, Wang H, Zhao Y, Wang Z, and Li F (2016). PRDM16 is associated with evasion of apoptosis by prostatic cancer cells according to RNA interference screening. Mol. Med. Rep 14, 3357–3361. 10.3892/mmr.2016.5605. [PubMed: 27511603]

## Highlights

- KU70 is a non-histone substrate of SETD4 methyltransferase
- Human KU70 is methylated at amino-acid residue K570
- Methylated KU70 is enriched in the cytoplasm and suppresses apoptosis

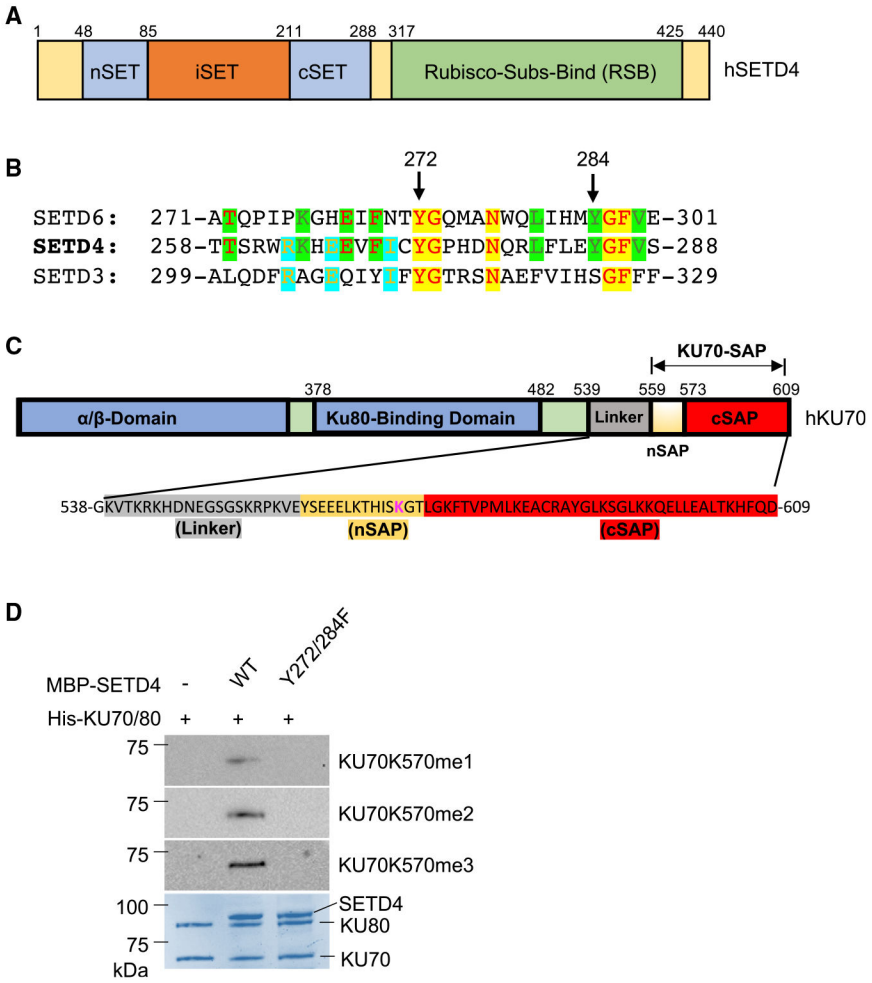


**Figure 1. Methylation of KU70 by SETD4 *in vitro***

(A) Domain structure of human SETD4. The SET domain of SETD4 is split into the nSET and cSET regions by an insert (iSET). The substrate-binding domain (Rubisco-Subs-Bind [RSB]) is located at the C terminus. Illustrated are the locations of predicted nSET, iSET, cSET, and RSB domains of SETD4.

(B) Amino-acid alignment of human SETD4 with SETD3 and SETD6 in the region containing tyrosine residues Y272 and Y284 of the putative active center in SETD4.

(C) Schematic domain structure of human KU70. Expanded is the C-terminal region containing a linker region (aa 539–558, marked in gray) and the commonly called KU70-SAP domain (aa 559–609). The C terminus 37 amino acids (aa 573–609, marked in red) of KU70, defined in the canonical SAP motif, are referred here as KU70-cSAP. The remaining 14 amino acids (aa 559–572, marked in yellow) are hereby referred as the nSAP of KU70.

(D) *In vitro* KU70 methylation by SETD4. Four mg of recombinant His-KU70/KU80 was incubated with 2 μg of MBP-SETD4 (WT) or a SETD4 mutant (Y272/284F) in the presence of SAM at 30°C for 2 h and then 65°C for 20 min. The mono-, di-, and tri-methylated KU70-K570 were detected with specific antibodies as characterized in Figure S2A. Coomassie-blue staining (bottom panel) was used to visualize the total amount of

KU70, KU80, and SETD4 proteins in the reactions. Shown are representative results of three independent experiments.

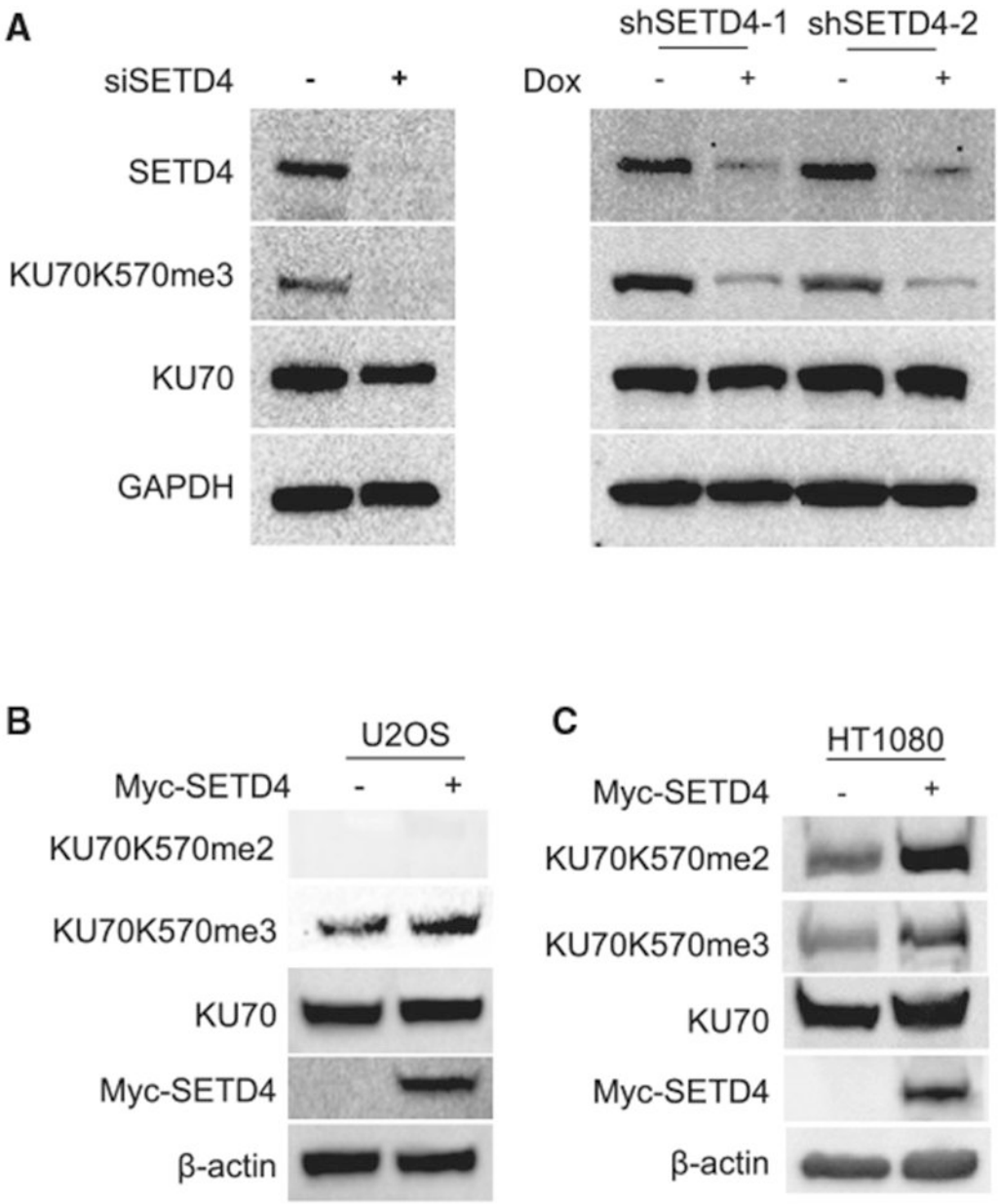


**Figure 2.** ***In vivo*** **KU70 methylation by SETD4**

(A) Knockdown of endogenous SETD4 reduced the level of tri-methylated KU70 (KU70K570me3). A transient siRNA transfection (left panel) and two inducible shRNA expression (right panel) approaches were used to target three independent regions of the SETD4 mRNA in H1299 cells. Cell extracts were analyzed by western blot to detect the endogenous SETD4, KU70K570me3, and total KU70. GAPDH was blotted as a loading control. Shown are represented results of three independent experiments. The sequences of siSETD4, shSETD4-1, and shSETD4-2 are shown in the key resources table. The quantifications of repeated experiments as represented here can be seem in Figures S4A and S4B.

(B and C) Over-expression of exogenous Myc-SETD4 enhances endogenous KU70K570me3. Exogenous Myc-SETD4 was stably expressed by transfection of pLXSH-Myc-SETD4 in U2OS (B) or HT1080 (C) cells. Total cell extracts were used to detect the endogenous levels of KU70K570me2, KU70K570me3, total KU70, and β-actin (loading control). Shown are representative results of three independent experiments. The quantifications of repeated experiments as represented here can be seem in Figures S4C-S4F.

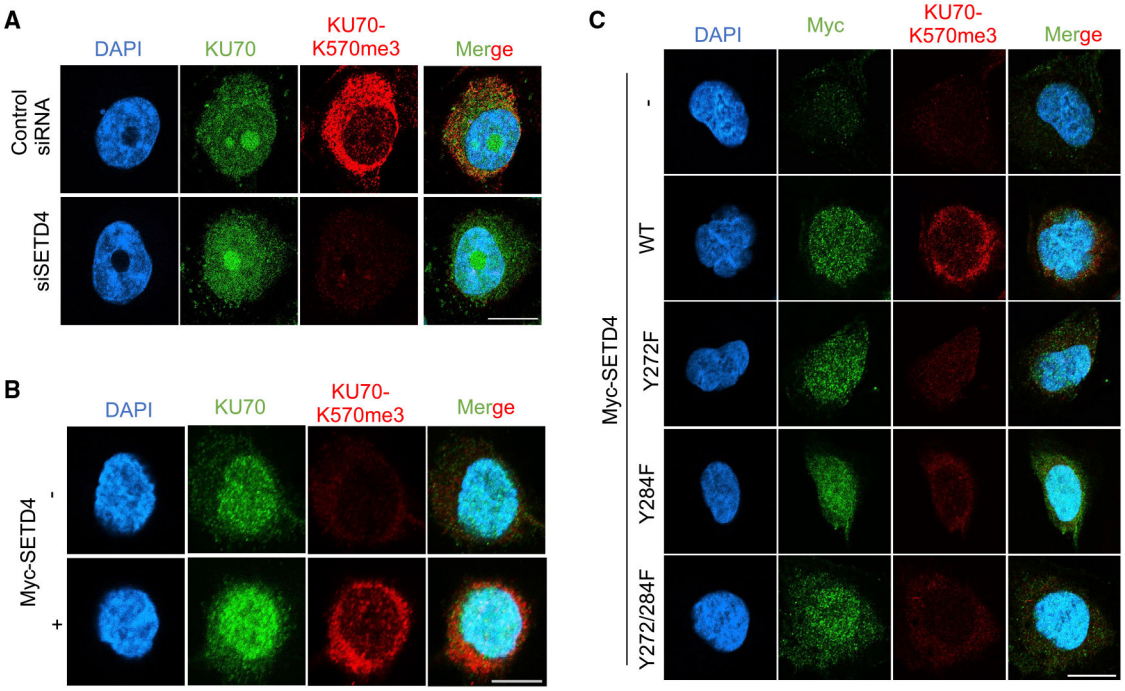


**Figure 3. Enrichment of methylated KU70 in the cytoplasm**

Images were obtained at a 0.3-μm thickness per slice using the Nikon A1R-Si Confocal Microscope System. Scale bar: 10 μm. Shown are images of representative cells. The quantifications of mean fluorescence from more than 50 cells of each group are shown in Figure S5, and additional images are shown in Figure S6.

(A) Knockdown of SETD4 reduced the endogenous KU70K570me3 that are enriched in the cytoplasm. After transient transfection with siSETD4 or control siRNA, two-colored IF staining was performed to visualize the levels and location of total KU70 (green) and KU70K570me3 (red) in H1299 cells. DAPI (blue) staining was used to visualize the nucleus.

(B and C) Overexpression of SETD4 enhanced endogenous KU70K570me3 in the cytoplasm. pLXSH retroviral vector was used to transmit cDNA into U2OS to stably express WT or mutant SETD4 proteins. Two-colored IF staining was performed to concurrently visualize the total KU70 (green, B) or Myc-SETD4 (green, C) and the endogenous KU70K570me3 (red, B and C).

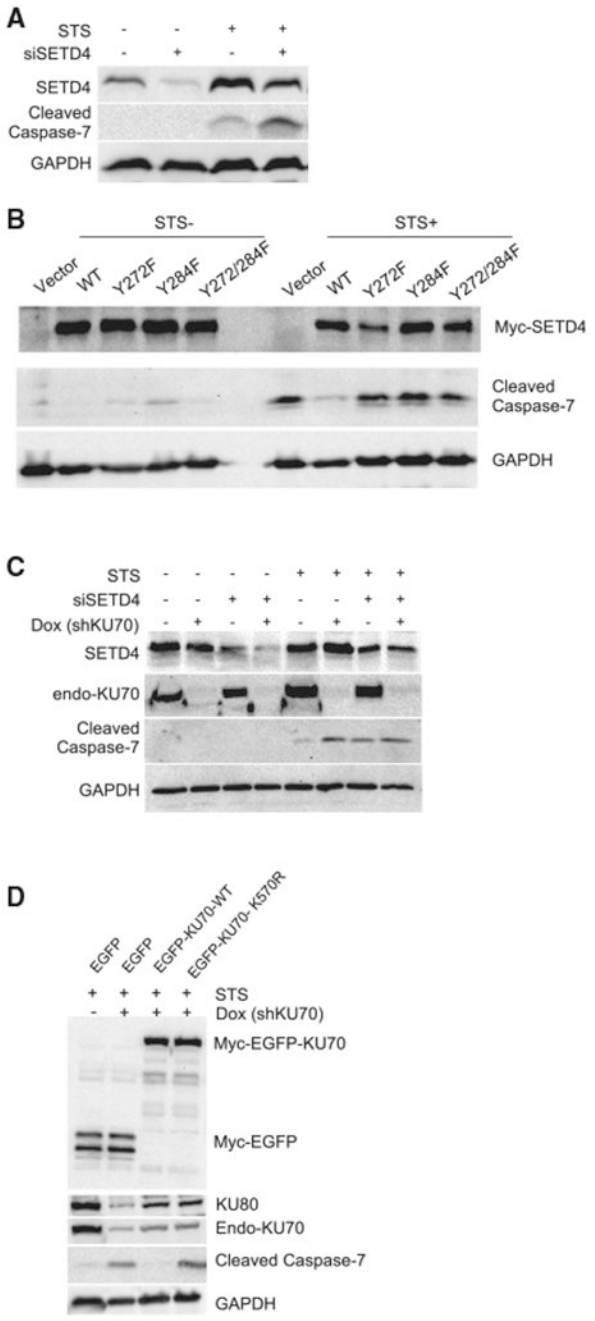


**Figure 4. SETD4 suppresses STS-induced apoptosis**

The cleaved caspase-7 was used as the marker for apoptosis and measured by immune-blot analysis after treatment with or without STS at 1 μM for 4 hrs. GAPDH was used as a loading control. Shown are representative results from 3 independent experiments, whose quantifications are summarized in Figures S7.

(A) Knockdown of SETD4 increases the apoptotic response to STS treatment. Forty-eight h after the H1299 cells were transfected with siRNA against SETD4 (siSETD4), the cells were treated with or without STS, and whole-cell extracts were collected for western blot.

(B) Over-expression of WT SETD4 suppresses STS-induced apoptosis. After the WT and mutant SETD4 were over-expressed, U2OS cells were treated with or without STS, and the cell extracts were used to detect apoptotic response. The specific forms of over-expressed SETD4 are labeled on the top of the panels.

(C) KU70 and SETD4 knockdowns have similar level of apoptosis. The shRNA-mediated knockdown of the endogenous KU70 in H1299 cells were induced by Dox treatment. siSETD4 were transfected to induce SETD4 knockdown. After KU70 and/or SETD4 knockdown were established, cells were treated with or without STS, and cleaved caspase-7 was detected.

(D) Re-expression of WT KU70, but not KU70-K570R, can dampen the elevated level of apoptosis in KU70-deficient H1299 cells. The Myc-EGFP and Myc-EGFP-tagged KU70-WT and KU70-K570R mutant were expressed in an H1299 cell line that had been installed with a Dox-inducible shKU70 expression. The cells were exposed with Dox to induce KU70 knockdown, were treated with STS, and were to detect the apoptotic response. The level of endogenous KU70 and KU80 were also monitored. See Figure S8 for similar experiments with A549 cells.

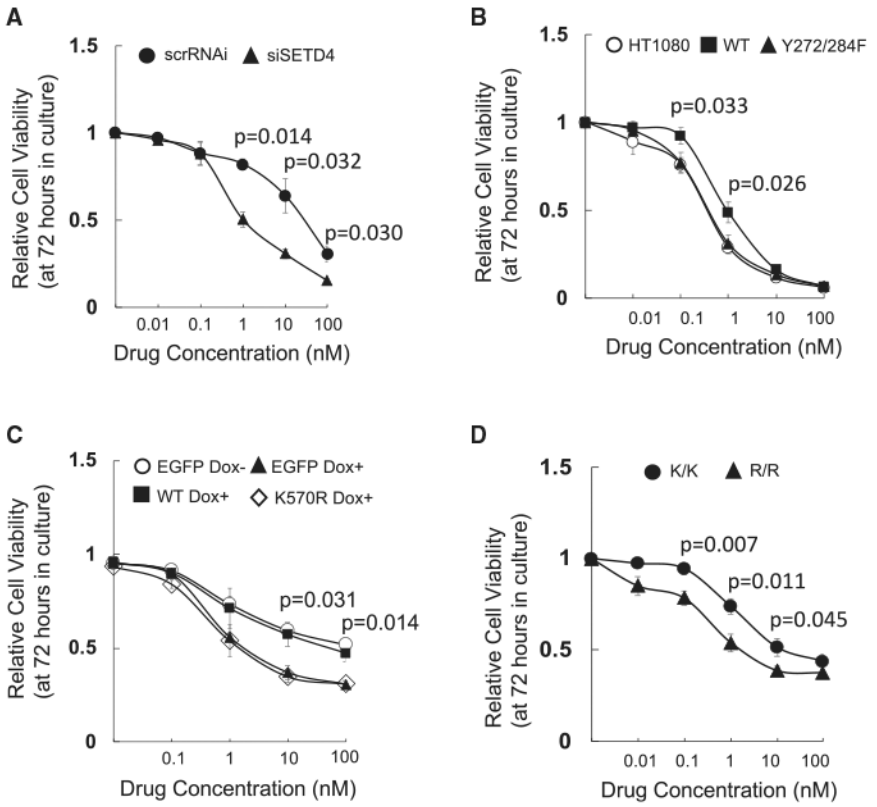


**Figure 5. Effects of SETD4 and KU70 deficiencies on cell growth in response to STS**

Individual cell lines as specified in each panel were cultured in the presence of indicated concentrations of STS. The viability of each group was recorded by the IncuCyte live-cell imager every 2 h. Shown are the relative viability at 72 h after continuous STS exposure, as normalized to the same cells without STS treatment. Results were the average of at least six independent experiments. Error bars are the standard errors of the means (SEMs). p values were calculated based on two-tailed Student t test. The individual data points from independent experiments are provided in Figures S9 and S10.

(A) A549 cells were transiently transfected with scrRNAi (Control) or siRNA targeting endogenous SETD4 (siSETD4). Seventy-two h after the transfection, the cells were continuously exposed to STS at the indicated concentrations.

(B) WT or mutant (Y272/284F) Myc-SETD4 were stably over-expressed in HT1080 that have modest level of endogenous SETD4. After 72 h of exposure to the indicated concentration of STS, the relative cell viabilities were quantified and plotted.

(C) Myc-EGFP-tagged KU70-WT or KU70-K570R mutant were stably expressed in an A549 cell line that had previously been established with a Dox-inducible KU70 knockdown. After treating the cells with Dox for 3 days, the cells were exposed to STS for another 72 h, and the relative cell viabilities during this period of 72 h were quantified and plotted. The p values refer to results of two-tailed Student t tests between WT Dox+ and K570R Dox+ at 10 and 100 nM, respectively.

(D) The MEFs were established from embryos of littermates upon a cross between heterozygous KU70-K568R mice. Shown are the relative cell viabilities of WT KU70 (K/K) and homozygous KU70-K568R mutant (R/R) MEFs upon exposure to STS for 72 h. The

averages of 2 MEF lines from each genotype were presented. See Figure S11 for related information.

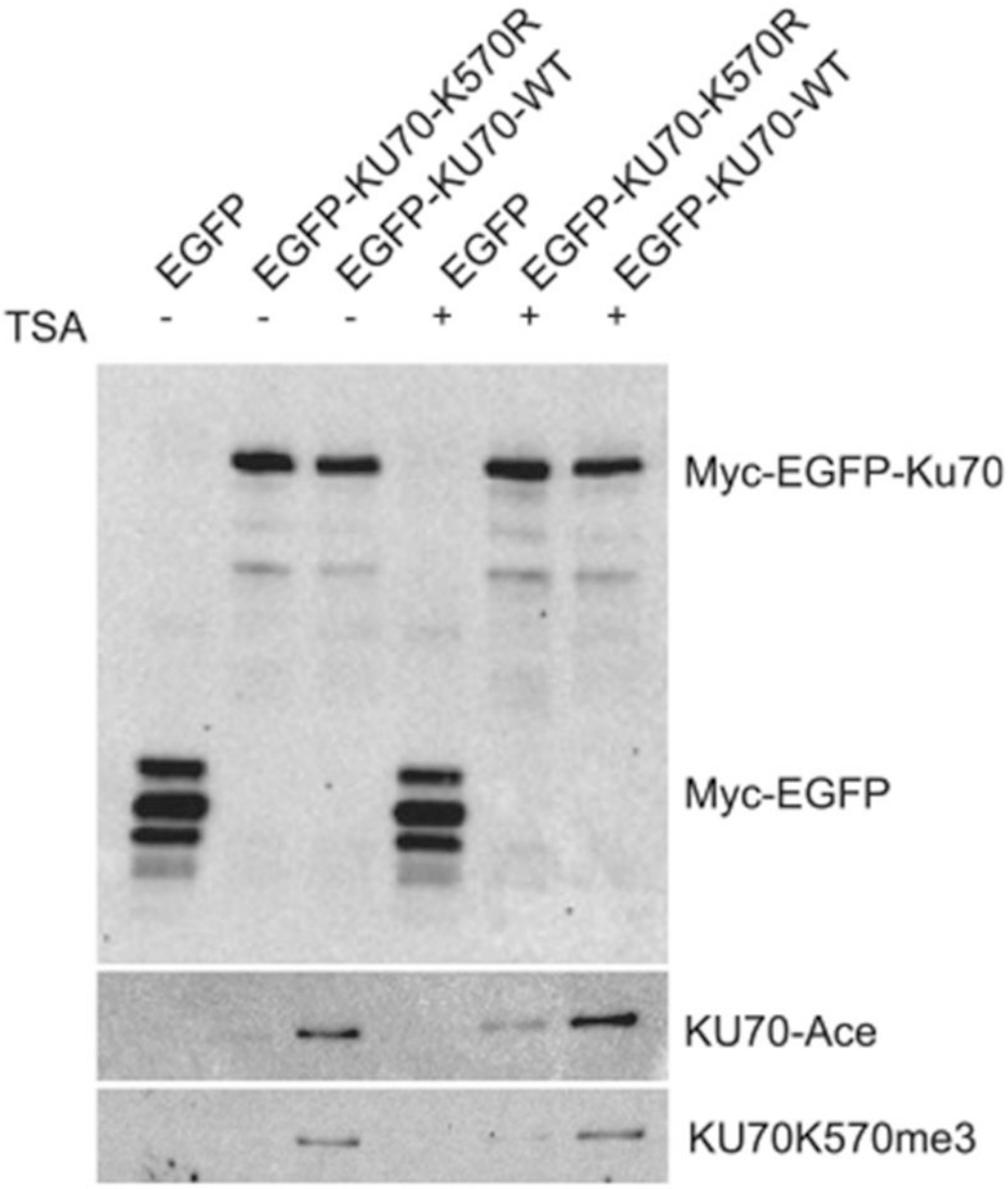


**Figure 6. KU70 methylation at K570 is required for KU70 acetylation**

H1299 cells stably overexpressing Myc-EGFP-tagged KU70-WT or KU70-K570R mutant were treated with or without deacetylase inhibitor trichostatin A (TSA) for 5 h. Myc-EGFP was used as a control. Cell lysates were immunoprecipitated using anti-Myc affinity beads and blotted with specific anti-KU70 methylation at K570 and pan acetyl-lysine antibodies, respectively. Shown are representative results of three independent experiments. The amount of precipitated Myc-EGFP-KU70 can be used as the reference to normalize the relative level of KU70 methylation and acetylation. See Figure S12 for similar experiments with A549 cells.

## KEY RESOURCES TABLE

| REAGENT OR RESOURCE | SOURCE | IDENTIFIER |
|---|---|---|
| Antibodies | | |
| Rabbit polyclonal anti-SETD4 (h25) | This paper | N/A |
| Rabbit polyclonal antibodies against nonmethylated KU70 (28C6) | This paper | N/A |
| Rabbit polyclonal antibodies against mono-methylated KU70-(28C6-CT) | This paper | N/A |
| Rabbit polyclonal antibodies against di-methylated KU70 (29A1-CT) | This paper | N/A |
| Rabbit polyclonal antibodies against tri-methylated KU70 (29A3-CT) | This paper | N/A |
| Mouse monoclonal anti-GAPDH (6C5) | Santa Cruz | Cat#sc-32233; RRID:AB_627679 |
| Mouse monoclonal anti-Myc (9E10) | Santa Cruz | Cat#sc-40; RRID:AB_2857941 |
| Mouse monoclonal anti-β-actin | Sigma-Aldrich | Cat#A1978; RRID:AB_476692 |
| Mouse monoclonal anti-KU70 | BD Biosciences | Cat#611893; RRID:AB_399373 |
| Mouse monoclonal anti-KU80 | Santa Cruz | Cat#sc-5280; RRID:AB_672929 |
| Rabbit polyclonal anti-cleaved Caspase 7 (Asp198) | Cell Signaling Technology | Cat#9491; RRID:AB_2068144 |
| Anti-c-Myc Agarose affinity antibody | Sigma-Aldrich | Cat#A7470; RRID:AB_10109522 |
| Alexa Fluor Plus 488, Goat anti-Mouse IgG (H+L) | Thermo Fisher Scientific | Cat#A32723; RRID:AB_2866489 |
| Rhodamine Red-X (RRX) AffiniPure Donkey Anti-Rabbit IgG (H+L) | Jackson Immuno Research Lab | Cat#711-295-152;RRID:AB_2340613 |
| Goat anti-Mouse IgG (H+L) Cross-Adsorbed Secondary Antibody, HRP | ThermoFisher Scientific | Cat#31432; RRID:AB_228302 |
| Donkey anti-Rabbit IgG (H+L) Cross-Adsorbed Secondary Antibody, HRP | Thermo Fisher Scientific | Cat#31458; RRID:AB_228213 |
| Chemicals, peptides, and recombinant proteins | | |
| DAPI Fluoromount-G | SouthernBiotech | Cat#0100-20 |
| Doxycycline hyclate | Sigma-Aldrich | Cat#D9891 |
| Staurosporine | Sigma-Aldrich | Cat#569397 |
| Trichostatin A | Sigma-Aldrich | Cat#T-8552 |
| Amylose resin | NEB | Cat#E8021S |
| Lipofectamine RNAiMAX Reagent | Invitrogen | Cat#13778-075 |
| S-adenosylmethionine | NEB | Cat#B9003S |
| HMT Buffer | NEB | Cat#B0233S |
| SET7 Methyltransferase | NEB | Cat#M0233S |
| KU70-nSAP peptide containing K570: 559-YSEEELKTHISKGTLGKFT-577 | Customarily synthesized by Syd Labs Inc. | N/A |
| Purified KU70/KU80 dimer protein | PROSPEC | Cat#PRO-397 |
| HiFiCas9 | IDT | Cat#1081061 |
| Critical commercial assays | | |
| Site-directed mutagenesis kit | NEB | Cat#E0554S |
| Deposited data | | |
| 3SMT:Crystal structure of human SETD3 | PDB | http://doi.org/10.2210/pdb3smt/pdb |
| 1JJR: The 3D structure of the C-terminal DNA Binding Domain of KU70 | PDB | http://doi.org/10.2210/pdb1jjr/pdb |
| Experimental models: Cell lines | | |
| HT1080 cells | ATCC | Cat#CCL-121 |
| U2OS cells | ATCC | Cat#HTB-96 |
| H1299 cells | ATCC | Cat#CRL-5803 |

| REAGENT OR RESOURCE | SOURCE | IDENTIFIER |
|---|---|---|
| A549 cells | ATCC | Cat#CRM-CCL-185 |
| HepG2 cells | ATCC | Cat#HB-8065 |
| MCF-7 cells | ATCC | Cat#CRL-3435 |
| HeLa | ATCC | Cat#CCL-2 |
| HEK293 cells | ATCC | Cat#CRL-1573 |
| HEK293T cells | ATCC | Cat#CRL-3216 |
| Phenix AMPH cells | ATCC | Cat#CRL-3213 |
| Mouse embryonic fibroblasts (MEF) | This paper | N/A |
| Experimental models: Organisms/strains | | |
| Mouse: Ku70$^{K568R/K568R}$: C57/BL6 | This paper | N/A |
| Oligonucleotides | | |
| siRNA against SETD4: 5'- GAGGGCUGAUGAGUCAAACAU-3' | Customary synthesized by Sigma-Aldrich | N/A |
| shRNA against SETD4 (shSETD4-1): 5'- AUUUCAGAAAAAAGAAACUA −3' | Customary synthesized by Sigma-Aldrich | N/A |
| shRNA against SETD4 (shSETD4-2): 5'- UAGGAAGUUUCAAGAUUCA −3' | Customary synthesized by Sigma-Aldrich | N/A |
| shRNA against KU70: 5'- GGAAGAGUCUACCCGACAU −3' | Customary synthesized by Sigma-Aldrich | N/A |
| scramble control siRNA: 5'-UUCGAACGUGUCACGUCAA-3' | Customary synthesized by Sigma-Aldrich | N/A |
| CRISPR sgRNA sequence: 5'-GTTATCAGAAGAAGAGCTGA-3' | Customary synthesized | N/A |
| PAGE purified donor oligo sequence (changes in lower case) 5'-CCATGAGCCTTGCATATGT CCTTCAGTGTAGGTACAGTGAGCTTACCC AGTGTGCCgcgACGAAAATGGGCtTTCAGC TCTTCTTCTGATAACTCTACCTTGGGCTTTTTACTCGTAGAACCTTCATCA-3' | Customary synthesized and purified. | N/A |
| Recombinant DNA | | |
| psPAX2 | Gift from Didier Trono (http://n2t.net/addgene:12260) | Addgene, Cat#12260 |
| pMD2.G | Gift from Didier Trono (https://www.addgene.org/12259/) | Addgene, Cat#12259 |
| pLXSP-Myc-EGFP | This paper | N/A |
| pLXSH | This paper | N/A |
| Tet-pLKO-Neo | (Wiederschain et al., 2009) (https://www.addgene.org/21916/) | Addgene, Cat#21916 |
| pMAL-c2X | (Walker et al., 2010) https://www.addgene.org/75286/ | Addgene, Cat#75286 |
| Software and algorithms | | |
| I-TASSER ver 3.0 | https://zhanglab.dcmb.med.umich.edu/I-TASSER/ (Roy et al., 2010) | N/A |
| Rosetta-Dock ver 3.2 | https://www.rosettacommons.org/software/servers (Gray et al., 2003; Lyskov and Gray, 2008). | N/A |
| AutoDock Vina ver 4 | https://vina.scripps.edu/ (Trott and Olson, 2010). | N/A |
| AutoDock Tools | https://vina.scripps.edu/ (Sanner, 1999). | N/A |

| REAGENT OR RESOURCE | SOURCE | IDENTIFIER |
|---|---|---|
| PyMol ver 2.0 | https://pymol.org/2/ (DeLano, 2009) | N/A |